# FUZZY BASED NOVEL CONTROL STRATEGY FOR DFIG BASED WIND ENERGY CONVERSION SYSTEM WITH INTEGRATED ACTIVE FILTER CAPABILITIES

**B.VENKATA SAI KRISHNA , Sri M.MAHESH**
PG Scholar, Department of Electrical and Electronics Engineering, JNTU, Anantapur, Andhra Pradesh
Lecturer, Department of Electrical and Electronics Engineering, JNTU, Anantapur, Andhra Pradesh

**Abstract — In this project we are implementing the Doubly Fed Induction Generator (DFIG) with an integrated active filter capabilities by utilising Grid Side Converter. In the paper Wind Energy Conversion System which is denoted as the STATCOM is used to supply the harmonics even when wind turbine is in shutdown condition. The grid side converter helps in supplying the harmonics in addition to its slip power transfer. Therefore the rotor-side converter is utilized for gaining the maximum power extraction and to supply the needed amount of reactive power to the DFIG. Control methodologies of both GSC and RSC are explained. Fuzzy logic controller is also used as a control method in this project for the better and accurate performance. By using the MATLAB/ Simulink we can verify the proposed method of the DFIG based wind energy conversion system.**

**Index Terms — Doubly fed induction generator(DFIG), fuzzy controller, integrated active filter, nonlinear load, power quality, wind energy conversion system(WECS).**

## I. INTRODUCTION

Now-a-days, non-renewable energy sources are getting degraded and also environmental pollution problems are arising. Demand of power is going on increasing by the increasing level of utility of power. So the renewable sources are being utilized to meet the ever increasing energy demand. The cost of non renewable energy sources is increasing .As a result, Wind energy is taken into account to be one amongst the potential sources of fresh energy for the long run. The study owes and also the associated controllers area unit, thus, turning into a lot and a lot of importance with every passing day. Now-a-days, several complete load area units are powered by renewable supplies of energy. And controlling of this project is completed by using fuzzy controller.

The other main advantages of this renewable source are eco-friendliness and unlimited in nature. Therefore, the wind energy is the most preferred out of all renewable energy sources. In the initial days, wind turbines are used as fixed speed wind turbines with squirrel cage induction generator and condenser banks. Most of the wind turbines are fixed speed due to their simplicity and low price. By perceptive turbine characteristics, one will clearly determine that for extracting maximum power, the machine should run at variable rotor speeds at completely different wind speeds. Using trendy power electronic converters, the machine is able to run at adjustable speeds. Out of all variable speed wind turbines, doubly fed induction generators (DFIGs) are preferred due to their low price. The other advantages of this DFIG are the higher energy output, lower convertor rating, and better utilization of generators. These DFIGs additionally provide good damping performance for the weak grid. Independent control of active and reactive power is achieved by the decoupled vector control algorithm given. This vector control of such system is usually realized in synchronously rotating reference frame designed in either voltage axis or flux axis. During this work, the control of rotor-side convertor (RSC) is implemented in voltage-oriented reference system. Grid code necessities for the grid connection and operation of wind farms are mentioned . Response of DFIG-based wind energy conversion system (WECS) to grid disturbance is compared to the fixed speed WECS. As the wind penetration in the grid becomes significant, the utilization of variable speed WECS for supplementary jobs like power smoothening and

harmonic mitigation are mandatory additionally to its power generation. This power smoothening is achieved by including super magnetic energy storage systems as proposed. The other auxiliary services like reactive power requirement and transient stability limit are achieved by including static compensator (STATCOM).

A distribution STATCOM (DSTATCOM) let alone fly-wheel energy storage system is employed at the wind farm for mitigating harmonics and frequency disturbances. However, the authors have used two additional converters for this purpose. A super condenser energy storage system at the dc link of unified power quality conditioner (UPQC) is proposed for improving power quality and reliability. In above methods , the authors have used separate converters for compensating the harmonics and also for controlling the reactive power. However, in later stages, some of the researchers have changed the control algorithms of already existed DFIG converters for mitigating the power quality issues and reactive power compensation

By using RSC, reactive power control and harmonics compensation is obtained. Therefore, harmonics are injected from the RSC into the rotor windings which creates losses and noise in the machine. These totally different harmonics in rotating part may also produce mechanical unbalance. These methods increase the RSC rating. However ,harmonic compensation and reactive power control are done also by using GSC. Therefore, the harmonics are not passing through machine windings in all cases.

In this work, a new control algorithm for GSC is planned for compensating harmonics produced by nonlinear loads using an indirect current control. RSC is used for controlling the reactive power of DFIG. PWM pulses are generated without any error by exploiting the fuzzy controller. The opposite main advantage of planned DFIG is that it works as an energetic filter even once the turbine is in shutdown condition. Therefore, it compensates load reactive power and harmonics at turbine stalling condition. The dynamic performance of the planned DFIG is additionally defined for varied wind speeds and changes in unbalanced nonlinear loads at point of common coupling (PCC).

## II. SYSTEM CONFIGURATION AND OPERATING PRINCIPLE

In DFIG, the stator coil is directly connected to the grid as shown in Fig. 1. Fig. 1 shows a schematic diagram of the planned DFIG primarily based WECS with integrated active filter capabilities. Two back-to-back connected voltage source converters (VSCs) are placed between the rotor and thus the grid. Nonlinear loads are connected at PCC as shown in Fig. 1. The planned DFIG works as an active filter additionally to the active power generation similar to traditional DFIG.

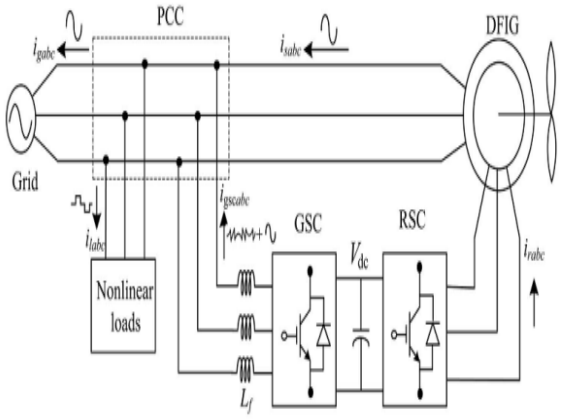


**Fig. 1. Proposed system configuration**

Harmonics generated by the nonlinear load connected at the PCC disturb the PCC voltage. These nonlinear load harmonic currents are mitigated by GSC control, so that the stator coil and grid currents are harmonic-free. RSC is controlled for achieving maximum power point tracking (MPPT) and additionally for creating unity power factor at the stator coil using voltage-oriented reference frame. Synchronous reference frame (SRF) control methodology is used for extracting the fundamental component of load currents for the GSC control.

## III. DESIGN OF DFIG-BASED WECS

Selection of ratings of VSCs and dc-link voltage is extremely much important for the successful operation of WECS. The ratings of DFIG and dc machine used in this experimental system are given in Appendix. in this section, a detailed style of VSCs and dc-link voltage is discussed

### A .Selection of DC-Link Voltage

The selection of dc-link voltage depends on both rotor voltage and PCC voltage. While considering from the rotor side, the rotor voltage is slip times the stator voltage. DFIG used in this experimental setup has stator to rotor turns ratio as 2:1. Normally, the DFIG operating slip is ±0.3. So, the rotor voltage is always less than the PCC voltage.

So, the design criteria for the selection of dc-link voltage is obtained by considering only PCC voltage. While considering from the GSC side, the PCC line voltage (Vab) is 230 V, as the machine is connected in delta mode. Therefore, the dc-link voltage is estimated as

$$V_{dc} \geq \frac{2\sqrt{2}}{\sqrt{3}*m} V_{ab} \qquad (1)$$

where Vab is the line voltage at the PCC. Maximum modulation index is selected as 1 for linear range. The value of dc-link voltage (Vdc) by (1) is selected as 375V.

### B. Selection of VSC Rating

The lagging volt-ampere reactive (VAR) drawn by DFIG is for its excitation to build the rated air gap voltage. It is calculated from the machine parameters that the lagging VAR of 2 kVAR is required when it runs as a motor. In DFIG case, the operating speed range is 0.7 to 1.3 p.u. Therefore, the maximum slip (Smax) is 0.3. Reactive power of 600 VAR (Smax ∗ Qs= 0.3 ∗ 2 kVAR) is needed from the rotor side (Q rmax) for making unity power factor at the stator side. The maximum rotor active power is (Smax ∗ P). The power rating of the DFIG is 5 kW. Therefore, the maximum rotor active power (Prmax) is 1.5 kW (0.3 ∗ 5 kW = 1.5 kW). So, the rating of the VSC used as RSC Srated is given as

$$S_{rated} = \sqrt{P_{r\,max}^2 + Q_{r\,max}^2} \qquad (2)$$

Thus, kVA rating of RSC Srated is calculated as 1.615 kVA.

### C. Design of Interfacing Inductor

The design of interfacing inductors between GSC and PCC depends upon allowable GSC current limit (igscpp), dc-link voltage, and switching frequency of GSC.Maximum line current depends upon the maximum power and the line voltage at GSC. The maximum possible power in the GSC is the slip power. In this case, the slip power is 1.5 kW. Line voltage (VL) at the GSC is 230 V (the machine is connected in delta mode). So, the line current is obtained as I gsc = 1.5 kW/(√3 ∗ 230) = 3.765 A. Considering the peak ripple current as 25% of rated GSC current, the inductor value is calculated as

$$L_i = \frac{\sqrt{3} m v_{dc}}{12 a f_m \Delta i_{gsc}} \qquad (3)$$

$$= \frac{\sqrt{3}\times 1\times 375}{12\times 1.5\times 10000\times 0.25\times 3.76} = 3.8\text{mH}.$$

Interfacing inductor between PCC and GSC is selected as 4 mH.

## IV. CONTROL STRATEGY AND SIMULATION RESULTS

Control algorithms for both GSC and RSC are presented in this section. Complete schematic control is given in Fig. 2. The control algorithm for emulating wind turbine characteristics using dc machine and Type A chopper is also shown in Fig. 2.

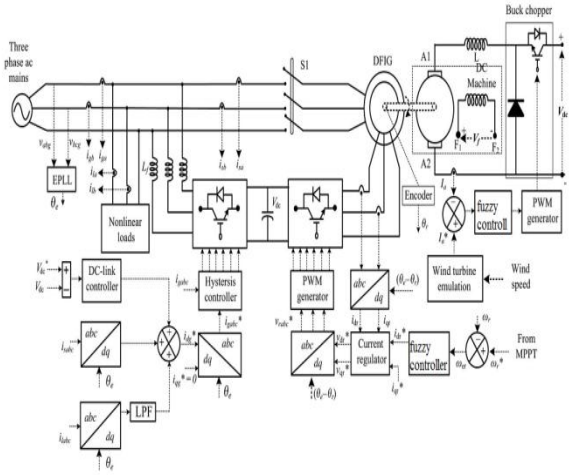


**Fig. 2. Control algorithm of the proposed WECS.**

### A. Control of RSC

Direct axis reference rotor current is selected such that maximum power is extracted for a particular wind speed. This can be achieved by running the DFIG at a rotor speed for a particular wind speed. Therefore, the outer loop is selected as a speed controller for

$$i_{dr}^*(k) = i_{dr}^*(k-1) + k_{pd}\{\omega_{er}(k) - \omega_{er}(k-1)\} + k_{id}\omega_{er}(k) \qquad (4)$$

where the speed error (ωer) is obtained by subtracting sensed speed (ωr) from the reference speed (ωr∗). kpd and kid are the proportional and integral constants of the speed controller. ωer(k) and ωer(k − 1) are the speed errors at kth and (k−1)th instants. i*dr(k) and i*dr(k − 1) are the direct axis rotor reference current at kth and (k−1)th instants. Reference rotor speed (ωr∗) is estimated by optimal tip speed ratio control for a particular wind speed.

Here, the RSC is controlled in voltage-oriented reference frame. Therefore, the active and reactive powers are controlled by controlling direct

and quadrature axis rotor currents (idr and iqr), respectively achieving direct axis reference rotor current (i∗dr) as inner current control loops are taken for control of actual direct and quadrature axis rotor currents (idr and iqr) close to the direct and quadrature axis reference rotor currents (i∗dr and i∗ qr). The rotor currents idr and iqr are calculated from the sensed rotor currents (ira, irb, and irc) as

$$i_{dr} = 2/3\left[i_{ra}\sin\theta_{slip} + i_{rb}\sin(\theta_{slip} - 2\pi/3) + i_{rb}\sin(\theta_{slip} - 2\pi/3)\right] \quad (5)$$

$$i_{qr} = 2/3\left[i_{ra}\cos\theta_{slip} + i_{rb}\cos(\theta_{slip} - 2\pi/3) + i_{rb}\cos(\theta_{slip} - 2\pi/3)\right] \quad (6)$$

where slip angle (θslip) is calculated as

$$\theta_{slip} = \theta_e - \theta_r \quad (7)$$

where θe is calculated from PLL for aligning rotor currents into voltage axis. The rotor position (θr) is achieved with an encoder.

Direct and quadrature axis rotor voltages (v'dr and v'qr ) are obtained from direct and quadrature axis rotor current errors (ider and iqer) as

$$v'_{dr}(k) = v'_{dr}(k-1) + k_{pdv}\{i_{der}(k) - i_{der}(k-1)\} + k_{idv}i_{der}(k) \quad (8)$$

$$v'_{qr}(k) = v'_{qr}(k-1) + k_{pdv}\{i_{qer}(k) - i_{qer}(k-1)\} + k_{iqv}i_{qer}(k) \quad (9)$$

where

$$i_{der} = i^*_{dr} - i_{dr} \text{ and } i_{qer} = i^*_{qr} - i_{qr} \quad (10)$$

where kpdv and kidv are the proportional and integral gains of direct axis current controller.

kpqv and kiqv are the proportional and integral gains of quadrature axis current controller. Direct and quadrature components are decoupled by adding some compensating terms as

$$v^*_{dr} = v'_{dr} + (\omega_e - \omega_r)\sigma L_r i_{dr} \quad (11)$$

$$v^*_{qr} = v'_{qr} - (\omega_e - \omega_r)(L_m i_{dr} + \sigma L_r i_{dr}) \quad (12)$$

These reference direct and quadrature voltages (vdr∗ , vqr∗ ) are converted into three phase reference rotor voltages (vra∗ , vrb∗ , vrc∗ ) as

$$v^*_{ra} = v^*_{dr}\sin\theta_{slip} + v^*_{qr}\cos\theta_{slip} \quad (13)$$

$$v^*_{rb} = v^*_{dr}\sin(\theta_{slip} - 2\pi/3) + v^*_{qr}\cos(\theta_{slip} - 2\pi/3) \quad (14)$$

$$v^*_{rc} = v^*_{dr}\sin(\theta_{slip} - 2\pi/3) + v^*_{qr}\cos(\theta_{slip} - 2\pi/3) \quad (15)$$

These three phase rotor reference voltages (vra∗ , vrb∗, ,vrc∗) are compared with triangular carrier wave of fixed switching frequency for generating pulse-width modulation (PWM) signals for the RSC.

The tuning of fuzzy controllers used in both RSC and GSC are achieved using Ziegler Nichols method. Initially, kid value is set to zero and the value of kpd was increased until the response stars oscillating with a period of Ti. Now, the value of kpd is taken as 0.45 kpd and kid is taken as 1.2 kpd/Ti.

Normally, the quadrature axis reference rotor current (i∗qr) is selected such that the stator reactive power (Qs) is made zero. In this DFIG, quadrature axis reference rotor current (i∗qr) is selected for injecting the required reactive power.

### B. Control of GSC

The novelty of this work lies in the control of this GSC for mitigating the harmonics produced by the nonlinear loads.

The control block diagram of GSC is shown in Fig. 2. Here, an indirect current control i s applied on t he grid currents f or making them sinusoidal and balanced. Therefore, this GSC s upplies t he harmonics for making grid currents s inusoidal and balanced. Active power component of GSC current is obtained by processing the dc-link voltage error (vdce) between reference and estimated dc-link voltage (Vdc∗ and Vdc) through fuzzy controller as

$$i^*_{gsc}(k) = i^*_{gsc}(k-1) + k_{pdc}\{v_{dce}(k) - v_{dce}(k-1)\} + k_{idc}v_{dce}(k) \quad (16)$$

where kpdc and kidc are proportional and integral gains of dc-link voltage controller. Vdce(k) and Vdce(k − 1) are dclink voltage errors at kth and (k−1)th instants. i∗gsc(k) and i∗gsc(k − 1) are active power component of GSC current at kth and (k−1)th instants.

Active power component of stator current (ids) is obtained from the sensed stator currents (isa, isb, and isc) using abc to dq transformation as

$$i_{ds} = 2/3\left[i_{sa}\sin\theta_e + i_{sb}\sin(\theta_e - 2\pi/3) + i_{sc}\sin(\theta_e + 2\pi/3)\right] \quad (17)$$

Fundamental active load current (il̇d) is obtained using SRF theory. Instantaneous load currents (ilabc) and the value of phase angle from EPLL are used for converting the load currents in to synchronously rotating dq frame (ild). In synchronously rotating frames, fundamental frequency currents are converted into dc quantities and all other harmonics are converted into non-dc quantities with a frequency shift of 50 Hz.

DC values of load currents in synchronously rotating dq frame (ild) are extracted using low-pass filter (LPF). Direct axis component of reference grid current (i∗gd) is obtained from the direct axis current of stator current (ids) and load current (ild) in synchronously rotating frame and the loss component of GSC current (i∗gsc) as

$$i_{gd}^{*} = i_{gsc}^{*} + i_{ds} - \overline{i_{ld}} \quad (18)$$

Quadrature axis component of reference grid current (i∗gq) is selected as zero for not to draw any reactive power from grid.

The hysteresis current controller is used to generate switching pulses for the GSC. The hysteresis controller is a feedback current control where sensed current tracks the reference current within a hysteresis band (ihb) [34]. At every sampling instant, the actual current (igabc) is compared to the reference current (i∗gabc) as

$$\Delta i_{gabc} = i_{gabc}^{*} - i_{gabc} \quad (19)$$

when $\Delta i_{gabc} > i_{hb}$ lower switch is turned ON (20)

when $\Delta i_{gabc} > i_{hb}$, upper switch is turned ON (21)

Using these equations, gating pulses for three phases of GSC are generated in the same way.

**Simulation Results**

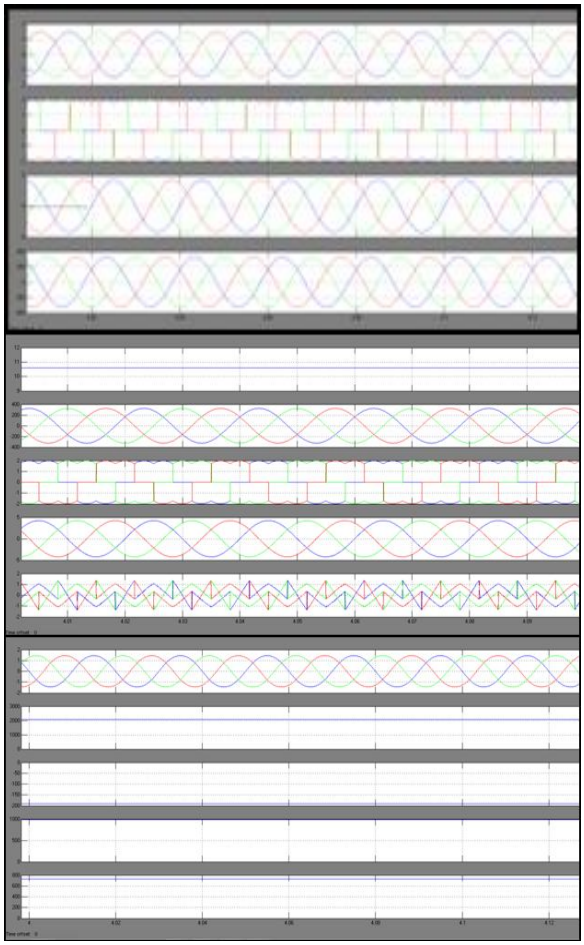

Fig. 3. Simulated performance of the proposed DFIG-based WECS at fixed wind speed of 10.6m/s (rotor speed of 1750rpm ).

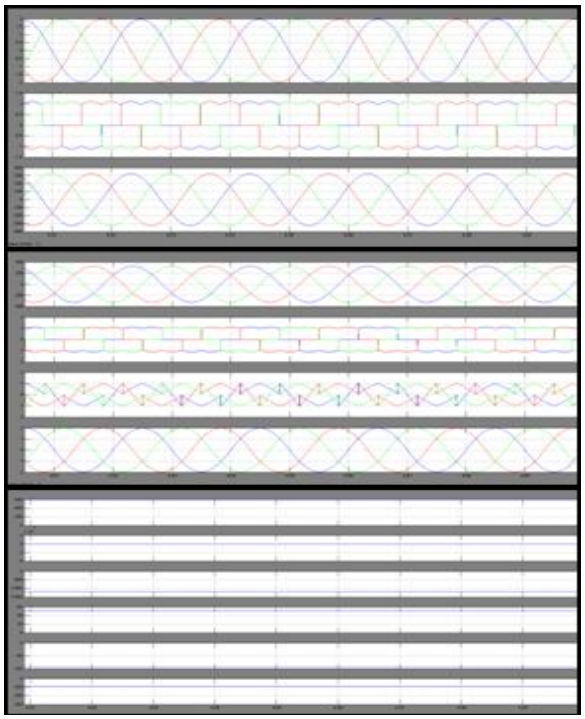

Fig. 4. Simulated performance of the proposed DFIG-based WECS working as a STATCOM at zero wind speed.

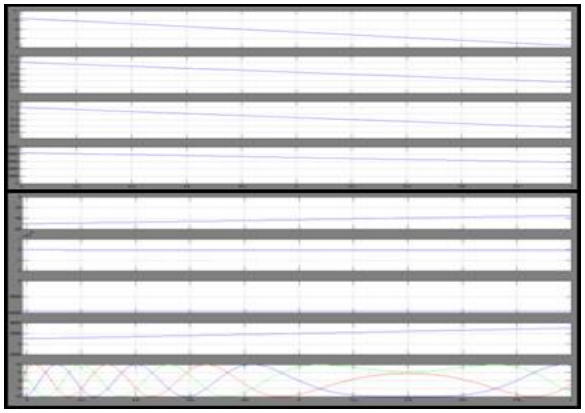

Fig. 5. Simulated performance of proposed DFIG for fall in wind speed.

## V. FUZZY LOGIC CONTROLLER

In FLC, basic control action is determined by a set of linguistic rules. These rules are determined by the system. Since the numerical variables are converted into linguistic variables, mathematical modeling of the system is not required in FC.

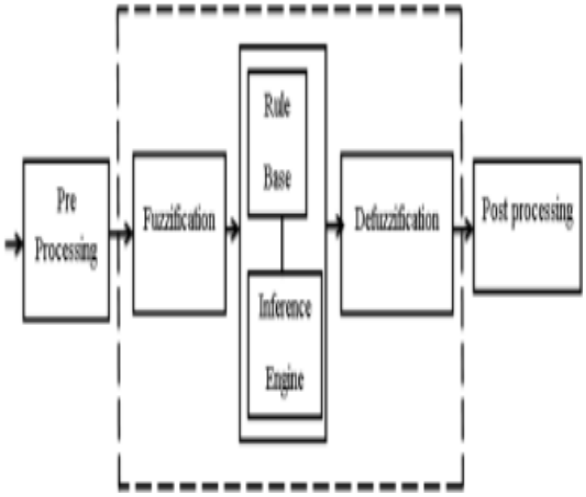


Fig.6.Fuzzy logic controller

The FLC comprises of three parts: fuzzification, interference engine and defuzzification. The FC is characterized as i. seven fuzzy sets for each input and output. ii. Triangular membership functions for simplicity. iii. Fuzzification using continuous universe of discourse. iv. Implication using Mamdani's, 'min' operator. v. Defuzzification using the height method.

**TABLE II** Fuzzy Rules

| Change in error | Error | | | | | | |
|---|---|---|---|---|---|---|---|
| | NB | NM | NS | Z | PS | PM | PB |
| NB | PB | PB | PB | PM | PM | PS | Z |
| NM | PB | PB | PM | PM | PS | Z | Z |
| NS | PB | PM | PS | PS | Z | NM | NB |
| Z | PB | PM | PS | Z | NS | NM | NB |
| PS | PM | PS | Z | NS | NM | NB | NB |
| PM | PS | Z | NS | NM | NM | NB | NB |
| PB | Z | NS | NM | NM | NB | NB | NB |

**Fuzzification:** Membership function values are assigned to the linguistic variables, using seven fuzzy subsets: NB (Negative Big), NM (Negative Medium), NS (Negative Small), ZE (Zero), PS (Positive Small), PM (Positive Medium), and PB (Positive Big). The Partition of fuzzy subsets and the shape of membership *CE(k) E(k)* function adapt the shape up to appropriate system. The value of input error and change in error are normalized by an input scaling factor.

In this system the input scaling factor has been designed such that input values are between -1 and +1. The triangular shape of the membership function of this arrangement presumes that for any particular *E(k)* input there is only one dominant fuzzy subset. The input error for the FLC is given as

$$E(k) = \frac{P_{ph(k)} - P_{ph(k-1)}}{V_{ph(k)} - V_{ph(k-1)}} \quad (22)$$

$$CE(k) = E(k) - E(k\text{-}1) \quad (23)$$

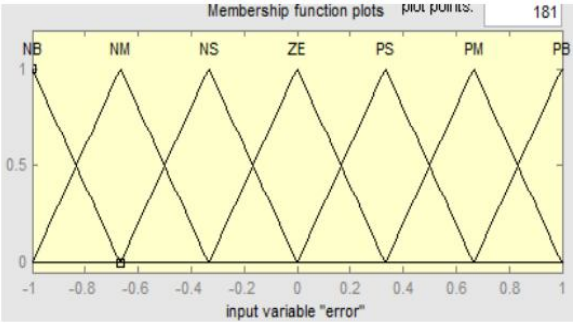


Fig.7.Membership functions

**Inference Method:** Several composition methods such as Max–Min and Max-Dot have been proposed in the literature. In this paper Min method is used. The output membership function of each rule is given by the minimum operator and maximum operator. Table 1 shows rule base of the FLC.

**Defuzzification:** As a plant usually requires a non-fuzzy value of control, a defuzzification stage is needed. To compute the output of the FLC, „height" method is used and the FLC output modifies the control output. Further, the output of FLC controls the switch in the inverter. In UPQC, the active power, reactive power, terminal voltage of the line and capacitor voltage are required to be maintained. In order to control these parameters, they are sensed and compared with the reference values. To achieve this, the membership functions of FC are: error, change in error and output.

The set of FC rules are derived from

$$u=-[\alpha E + (1-\alpha)*C] \quad (24)$$

where α is self-adjustable factor which can regulate the whole operation. E is the error of the system, C is the change in error and u is the control variable. A large value of error E indicates that given system is not in the balanced state. If the system is unbalanced, the controller should enlarge its control variables to balance the system as early as possible. On the other hand, small value of the error E indicates that the system is near to balanced state.

**TABLE I**
**CURRENT DISTORTION LIMITS FOR GENERAL DISTRIBUTION SYSTEMS IN TERMS OF INDIVIDUAL HARMONICS ORDER (ODD HARMONICS)**

| $I_{sc}/I_L$ | <11 | 11 ≤ h ≤17 | 17 ≤ h ≤ 23 | 23 ≤ h ≤ 35 | 35 ≤ h | TDD |
|---|---|---|---|---|---|---|
| < 20 | 4.0 | 2.0 | 1.5 | 0.6 | 0.3 | 5.0 |
| 20 < 50 | 7.0 | 3.5 | 2.5 | 1.0 | 0.5 | 8.0 |
| 50 < 100 | 10 | 4.5 | 4.0 | 1.5 | 0.7 | 12 |
| 100 < 1000 | 12 | 5.5 | 5.0 | 2.0 | 1.0 | 15.0 |
| > 1000 | 15.0 | 7.0 | 6.0 | 2.5 | 1.4 | 20.0 |

Maximum harmonic current distortion is in percent of IL. Isc = maximum short-circuit current at PCC; IL = maximum demand load current (fundamental frequency component) at PCC.

## VI. RESULTS AND DISCUSSION

Simulated results are presented in this section for validating steady-state and dynamic performances of this proposed DFIG with integrated active filter capabilities.

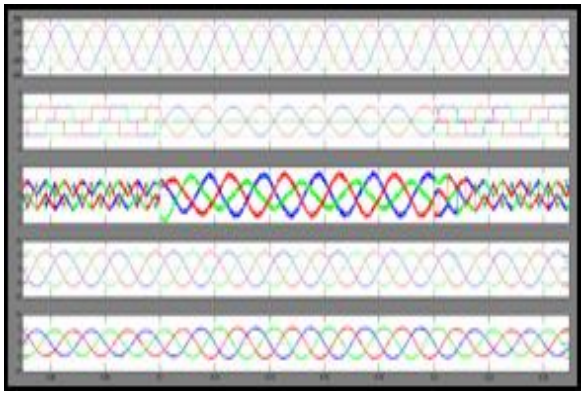

Fig. 8. Dynamic performance of DFIG-based WECS for the sudden removal and application of local loads.

## VII. CONCLUSION

In this projected DFIG, the reactive power for the induction machine has been provided from the RSC and the load reactive power has been supplied from the GSC.The grid side device control algorithm of this DFIG has been changed for supplying the harmonics and reactive power of the local loads.. Both active and reactive powers has been achieved by RSC control. The controlling for this device is completed by the fuzzy controller The projected DFIG has additionally been verified at turbine obstruction condition for compensating harmonics and reactive power of local loads. This proposed system with an integrated active filter has been simulated using MATLAB/Simulink environment. Dynamic performance of this proposed GSC control algorithm has also been verified for the variation in the wind speeds and for local nonlinear load.

## REFERENCES

[1] D. M. Tagare, Electric Power Generation the Changing Dimensions. Piscataway, NJ, USA: IEEE Press, 2011.

[2] G. M. Joselin Herbert, S. Iniyan, and D. Amutha, "A review of technical issues on the development of wind farms," Renew. Sustain. Energy Rev., vol. 32, pp. 619–641, 2014.

[3] I. Munteanu, A. I. Bratcu, N.-A. Cutululis, and E. Ceang, Optimal Control of Wind Energy Systems Towards a Global Approach. Berlin, Germany: Springer-Verlag, 2008.

[4] A. A. B. Mohd Zin, H. A. Mahmoud Pesaran, A. B. Khairuddin, L. Jahanshaloo, and O. Shariati, "An overview on doubly fed induction generators controls and contributions to wind based electricity generation," Renew. Sustain. Energy Rev., vol. 27, pp. 692–708, Nov. 2013.

[5] S. S. Murthy, B. Singh, P. K. Goel, and S. K. Tiwari, "A comparative study of fixed speed and variable speed wind energy conversion systems feeding the grid," in Proc. IEEE Conf. Power Electron. Drive Syst. (PEDS'07), Nov. 27–30, 2007, pp. 736–743.

[6] D. S. Zinger and E. Muljadi, "Annualized wind energy improvement using variable speeds," IEEE Trans. Ind. Appl., vol. 33, no. 6, pp. 1444– 1447, Nov./Dec. 1997.

[7] H. Polinder, F. F. A. van der Pijl, G. J. de Vilder, and P. J. Tavner, "Comparison of direct-drive and geared generator concepts for wind turbines," IEEE Trans. Energy Convers., vol. 21, no. 3, pp. 725–733, Sep. 2006.

[8] R. Datta and V. T. Ranganathan, "Variable-speed wind power generation using doubly fed wound rotor induction machine—A comparison with alternative schemes," IEEE Trans. Energy Convers., vol. 17, no. 3, pp. 414–421, Sep. 2002.

[9] E. Muljadi, C. P. Butterfield, B. Parsons, and A Ellis, "Effect of variable speed wind turbine generator on stability of a weak grid," IEEE Trans. Energy Convers., vol. 22, no. 1, pp. 29–36, Mar. 2007.

[10] R. Pena, J. C. Clare, and G. M. Asher, "Doubly fed induction generator using back-to-back PWM converters and its application to variable-speed wind-energy generation," IEE Proc. Elect. Power Appl., vol. 143, no. 3, pp. 231–241, May 1996.